Phase Transition at a Nanometer Scale Detected by Acoustic Emission within the Cubic Phase $Pb(Zn_{1/3}Nb_{2/3})O_3$-$x$$PbTiO_3$ Relaxor Ferroelectrics

Michael Roth,[1] Evgeny Mojaev,[1] Evgeniy Dul'kin,[1,*] Pascale Gemeiner,[2] and Brahim Dkhil[2]
[1] *Faculty of Science, The Hebrew University of Jerusalem, Jerusalem 91904, Israel*
[2] *Laboratoire Structures, Propriétés et Modélisation des Solides, CNRS-UMR 8580, Ecole Centrale Paris, 92295 Châtenay-Malabry cedex, France*

(Received 5 March 2007; published 27 June 2007)

$Pb(Zn_{1/3}Nb_{2/3})O_3$-$x$$PbTiO_3$ ($x = 4.5\%$–12%) relaxor ferroelectric crystals have been studied by means of acoustic emission (AE) in the 400–540 K temperature range. An anomalous AE activity independent of the ground state relaxor/morphotropic/ferroelectric crossover has been revealed at around 500 K, and it is associated with the "waterfall" feature related to the existence of polar nanoregions (PNRs). The 500 K AE anomaly is attributed to local martensitelike cubic-to-tetragonal ferroelectric transitions within the PNRs imbedded in a nonpolar (cubic) matrix.

DOI: 10.1103/PhysRevLett.98.265701 PACS numbers: 64.70.Kb, 62.65.+k, 77.84.Dy

Relaxor ferroelectrics, such as $Pb(Mg_{1/3}Nb_{2/3})O_3$ (PMN), $Pb(Zn_{1/3}Nb_{2/3})O_3$ (PZN), and related perovskite oxides, have recently attracted a great deal of attention due to the outstanding piezoelectric, dielectric, and electromechanical properties of their solid solutions with $PbTiO_3$ (PT) within the morphotropic phase boundary (MPB: 8%–11%PT at room temperature [1]) [2,3]. In relaxor materials, the temperature dependences of real and imaginary parts of the complex dielectric permittivity show high and broad maxima (T_m) that shift to higher temperatures with increasing the measurement frequency. Presently, it is generally accepted that strong dielectric dispersion of T_m is a consequence of the dynamics of polar nanoregions (PNRs), which nucleate several hundreds of degrees above T_m at the Burns temperature (T_d) [4]. At higher temperatures, relaxors exist in a nonpolar paraelectric phase, which is similar in many aspects to the paraelectric phase of normal ferroelectrics. Upon cooling they transform into the ergodic relaxor state in which PNRs with randomly distributed directions of dipole moments appear below T_d. The presence of PNRs is reflected in a number of physical phenomena, and among them in the acoustic emission (AE) [5].

Recently, we have shown that the AE method allows us to detect not only classical phase transitions in relaxor ferroelectrics, including those induced under external electric fields, but also broad anomalies related to the PNRs [6,7]. In particular, distinct AE responses presumably associated with PNRs have been revealed below the T_d and above the ferroelectric transition temperature, T_c, at around 500 K in both pure PZN and PZN-9.0PT crystals [6]. These results are quite intriguing as the two compounds exhibit different low temperature ground states (rhombohedral for PZN and monoclinic or orthorhombic for PZN-9.0PT), and yet the temperatures related to the existence of PNRs and occurring at around $T_d = 730$ K and at 500 K are nearly identical with or without Ti addition.

In the present work we investigate by means of the AE method a more extended part of the phase diagram of PZN-xPT ($x = 4.5$ to 12.0), including the crossover from relaxor to classical ferroelectric state through the MPB. More detailed information regarding the dependence of the peculiar high-temperature AE anomaly at around 500 K on the composition is very desirable as, eventually, it may shed new light on the path from relaxor state to the highly piezoelectric morphotropic systems at a nanometer scale. We propose to explain the AE radiation around 500 K by a local polar phase transition in the framework of the existing models of PNR dynamics.

{001}-cut single crystal plates ($3 \times 3 \times 0.3$ mm^3) of PZN-xPT ($x = 4.5$, 6.0, 7.0, 9.0, 12.0) were studied using the dedicated AE technique described in detail elsewhere [8]. Each sample was coupled with silver epoxy to the polished side of an acoustic silica waveguide. A PZT-19 piezoelectric sensor was attached to the rear end of the waveguide. The sensor was electrically coupled to a 500 kHz band pass low-noise variable preamplifier (up to 40 db) connected to an amplifier-detector (40 db). A Ch-Al thermocouple junction was glued to the waveguide near the sample. Both the thermocouple and amplifier outputs were interfaced with a PC. The sample with the adjacent part of the waveguide was mounted in a resistance element furnace. All samples were preheated to 540 K, and the AE count rate ($dN/dt = \dot{N}$, s^{-1}) was monitored in the 400–540 K temperature range at an average cooling rate of 1–3 K s^{-1}.

Figure 1 shows the AE activity, $\dot{N}$, as a function of temperature for PZN-4.5PT, PZN-6.0PT, PZN-7.0PT, PZN-9.0PT, and PZN-12.0PT crystals on cooling from 540 K. Two groups of AE peaks can be distinguished within the measured temperature range. The lower temperature group comprises AE peaks varying from 435 to 465 K with an increasing PT content. They correspond to the paraelectric (cubic) to ferroelectric (rhombohedral/orthorhombic or monoclinic/tetragonal)

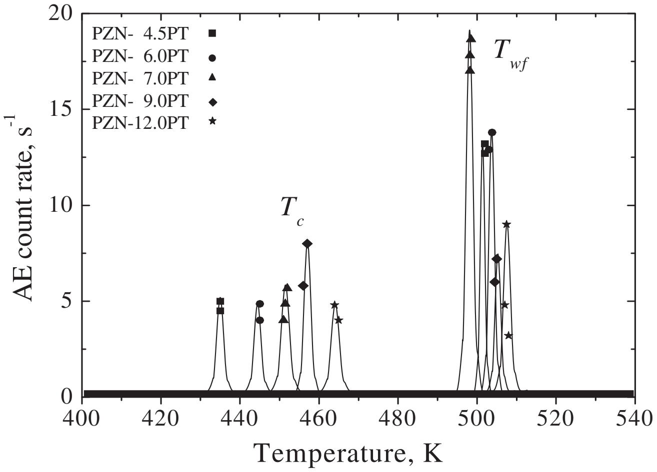

FIG. 1. AE activity as a function of temperature during cooling of PZN-xPT crystals (x values are indicated in the figure). The thick line at the bottom denotes the electronic noise level.

phase transition temperatures, T_c, dependent on the composition (PT content) in agreement with recent phase diagram [9]. The individual T_c values are listed in Table I together with our previously reported AE data on pure PZN and PZN-9.0PT crystals from a different batch. Generally, the bursts of AE at T_c are explained by formation of a ferroelectric twinned domain structure due to relaxation of mechanical stresses at the boundary between the paraelectric and ferroelectric phases [6].

In addition, Fig. 1 features a higher temperature group of $\dot{N}$ peaks which are densely spaced around 500 K (from 498 to 507 K; see also Table I) and are on the average more intense than the regular T_c peaks. Apparently, there is little correlation between the peak intensity and the crystal composition, which may be due to the sample-dependent concentrations of trace impurities and other defects influencing structural changes. Only a slight trend in the related AE peak location, towards higher temperatures with the PT-content increase, can be detected. We assume therefore that the anomalous AE activity appearing at 500 K in the macroscopically cubic paraelectric phase is very weakly dependent of the titanium addition. Formerly, we implied that the 500 K anomaly was related to the existence of PNRs [6] in both PZN and PZN-9.0PT. Our present results suggest that PNRs continue to exist even in PT-rich crystals (i.e., $x > 11\%$, beyond the MPB) where the relaxor behavior is thought to be suppressed. Indeed, the existence of PNRs has been shown to extend at least to the PZN-15.0PT composition [9].

TABLE I. Peak values of temperatures and acoustic emission activities related to the macroscopic ferroelectric and anomalous 500 K phase transitions. Earlier literature data transition temperatures are given for comparison.

Crystal	T_c, K	$\dot{N}_c$, s^{-1}	T_{wf}, K	$\dot{N}_{\mathrm{wf}}$, s^{-1}	Reference
PZN	413	-	505	-	[6]
PZN-9.0PT	455	-	507	-	
PZN-4.5PT	435	5.0	502	13.2	This work
PZN-6.0PT	445	4.9	504	13.8	
PZN-7.0PT	452	5.7	499	18.6	
PZN-9.0PT	457	8.0	505	7.2	
PZN-12.0PT	465	4.8	508	9.0	

The weak dependence of the 500 K anomaly on the PT content is most likely not accidental. It is interesting to note that the so-called "waterfall" phenomenon that has been initially discovered around the same temperature in PZN- and PMN-type relaxor ferroelectrics [10,11]. The waterfall is manifested by a precipitous drop of the transverse optical (TO) phonon branch (soft mode characteristic of normal ferroelectrics) into the lower transverse acoustic (TA) branch, which occurs at reduced wave vector values of about $q_{\mathrm{wf}} \sim 0.2$ Å^{-1} in PZN [12], PZN-8.0PT [10], and PZN-15.0PT [9]. It has been proposed that the large damping of TO modes is due to the presence of PNRs which prevent the propagation of phonons with wavelength larger than the size of the PNRs, and thus the wave vector q_{wf} is the measure of the average size of the PNRs [12]. It is noteworthy that according to Hlinka *et al.* [13], q_{wf} depends on the choice of the Brillouin zone and its relation to the size of PNRs is not straightforward. The waterfall is thus an apparent effect that can be explained by coupling of acoustic and optic phonon branches. Nevertheless, we assign for the sake of convenience the anomalous 500 K temperature as T_{wf}. The exact experimental values of T_{wf} obtained for samples studied hereby together with the earlier data [6] are given in Table I.

In order to elucidate the origin of the characteristic T_{wf} temperature, we briefly reflect on the dynamics of PNR evolution. At T_d or higher temperatures, polar order is developed in nanosize regions containing a few unit cells, while most (but not necessarily all [14]) of these unit cells are spontaneously polarized in one and the same direction. Upon cooling, the number of PNRs increases, but the equilibrium size of each of them does not change initially. In polycrystalline PZN, a tangible deviation of the cubic phase lattice constant from the normal thermal expansion behavior starts at a characteristic temperature $T_s = 550$ K as revealed by Iwase *et al.* [15] using the neutron powder diffraction technique. They show that the cumulative relative volume of PNRs is $>15\%$ at 500 K and reaches 40% at room temperature. A more detailed study of the PZN-xPT system has been carried out by La-Orauttapong *et al.* [16,17] by means of diffuse elastic neutron scattering. The width of the diffuse scattering peak, which is related to a correlation length, is shown to provide a measure of the PNR's size. They find that a relatively rapid increase in the correlation length (ξ), or average PNR size, begins at a similar characteristic temperature T^*, which marks the onset of condensation and eventual orientational (polarization) freezing of the PNRs on further temperature decrease.

The parallel rise in the diffuse scattering intensity, which is proportional to $\langle P_s^2\rangle$, indicates an increase in the net local polarization within the PNR. It has been also found that T^* is composition dependent (PZN: ∼450 K, PZN-4.5%PT: ∼500 K, PZN-9%PT: ∼550 K) [16,17]. However, a closer examination of the temperature dependences of the correlation lengths reveals that at 500 K they are of the order of $x_c = 25$–30 Å for all three compositions in scattering around the (011) and (100) Bragg reflections. If we presume that this average size of the PNRs is associated with a critical volume for local ferroelectric phase transitions, due to electrostrictive coupling between strain and polarization, the existence of a nearly constant $T_{\rm wf} \sim 500$ K can be understood. In fact, the cubic-to-tetragonal phase transformation at 500 K upon zero-field cooling has been detected by neutron diffraction measurements in PZN-8.0PT [18]. It is noteworthy that another characteristic temperature, T_d (not Burns temperature), has emerged from Raman spectra analysis of pure PZN in the 470–500 K range [19]. This temperature is claimed to mark the onset of local phase transformations and the appearance of strain fields at which PNRs actually form. Since the composition dependence of "T_d" has not been reported yet, it is premature to conclude how it relates to $T*$ and $T_{\rm wf}$.

The proposed model of local ferroelectric phase transitions in PNRs exceeding a critical volume explains also the nearly composition-independent AE activity at 500 K. The phase mismatch between the nascent ferroelectric nanodomains and the paraelectric matrix is apt to generate appreciable mechanical stresses at the PNR's boundaries. In order to minimize the accumulated elastic energy, the domains containing 7–8 unit cells may break down into a tetragonal nanotwin structure [20] for stress accommodation. This twinning produces changes in the internal strain field accompanied by generation and movement of dislocations at the PNR-matrix boundary, giving rise to elastic waves propagating within the crystal, or to AE around $T_{\rm wf}$ as shown in Fig. 1 for all PZN-xPT compositions. When formed through the high-temperature microscopic ferroelectric phase transitions, as suggested above, the static polar nanodomains presumably continue to exist below the macroscopic first-order phase transition at T_c (most likely, by heterogeneous nucleation on PNRs and growth). This was recently shown in the case of PMN-xPT materials [21,22], where $\langle 110\rangle_c$-oriented (tetragonal) nanotwins were observed within PNRs using the polarized light and transmission electron microscopy techniques.

The mechanism discussed above is similar to twinning of polarized embryos inside a paraelectric matrix through the displacive and, therefore, martensitelike ferroelectric phase transition in normal ferroelectrics [23,24]. The transition-related stress may be relaxed by breaking up these embryos into head-to-tail arranged 90°-domain twins. A schematic example is shown in Fig. 2, where a ferroelectric lamellar tetragonal twin is formed in a cubic paraelectric matrix. Tetragonal twins with 180° and 90° domain walls were observed using TEM in PZN-xPT crystals [25]. In order for the 90° twins to remain stabilized down to room temperature, the phase-mismatch-induced stresses must exceed the yield stresses, or the associated strain leaps must be equal or larger than certain values, $|\Delta\varepsilon_s| \geq |\Delta\varepsilon_s^0|$ [23,26]. We recall that $\Delta\varepsilon_s^0$ is electrostrictive in nature being due to the existence of spontaneous structural polarization. There are three components of such strain leaps in the tetragonal state, and they can be expressed by [23,27]

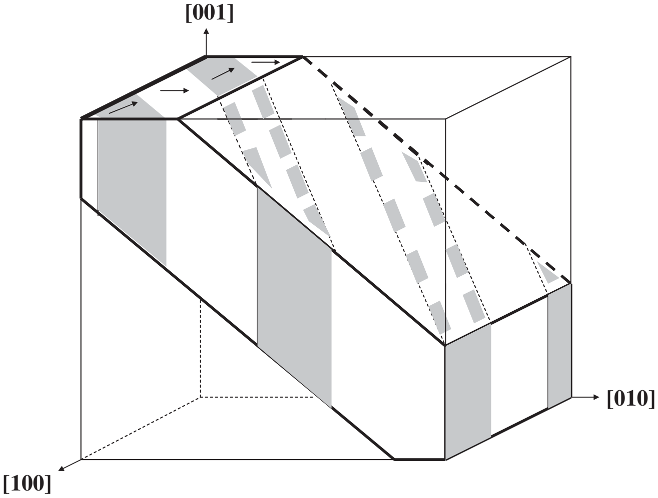

FIG. 2. Schematic representation of a twinned ferroelectric (tetragonal) domain in a paraelectric (cubic) matrix. Arrows denote head-to-tail polarization directions of 90° twins.

$$\Delta\varepsilon_{s1}^0 = \Delta\varepsilon_{s2}^0 = Q_{12}P_s^2 \quad \text{and} \quad \Delta\varepsilon_{s3}^0 = Q_{11}P_s^2, \tag{1}$$

where $\Delta\varepsilon_{s1}^0$, $\Delta\varepsilon_{s2}^0$ and $\Delta\varepsilon_{s3}^0$ are the induced transverse and longitudinal strain components, respectively, Q_{12} and Q_{11} are the relevant electrostrictive coefficients and P_s is the polarization along the $\langle 001\rangle$ direction. The appropriate phase-mismatch-induced strains are defined as [26]

$$\Delta\varepsilon_{s1} = \Delta\varepsilon_{s2} = a_t/a_c - 1 \quad \text{and} \quad \Delta\varepsilon_{s3} = c_t/a_c - 1, \tag{2}$$

where a_c is the cubic and a_t and c_t are the tetragonal lattice constants. For PZN-8.0PT, the extrapolated lattice constants at 500 K are: $a_c = 4.04$ Å and $a_t = 4.028$ Å [23], and the first of Eqs. (2) yields $\Delta\varepsilon_{s1} \approx -10^{-3}$. If we adopt the critical value of spontaneous polarization, $P_s = 0.13$ C/m^2, deduced for the cubic-to-tetragonal (ferroelectric) transformation in PZN [28] and $Q_{12} = -0.035$ m^4/C^2 in PZN-8.0PT [29], then $\Delta\varepsilon_{s1}^0 \approx -6 \times 10^{-4}$ from the first of Eqs. (1). Thus, the criterion $|\Delta\varepsilon_s| \geq |\Delta\varepsilon_s^0|$ is fulfilled, like in most classical ferroelectrics, such as PbTiO$_3$ and BaTiO$_3$ [23]. Consequently, the 90° twin domain structure may be formed within the PNRs at $T_{\rm wf}$ as it apparently occurs in PMN-xPT [22]. The sample calculation performed above merely demonstrates the feasibility of twinning in the tetragonal phase in consistence with the recent theoretical treatise [20].

More sophisticated criteria, or constraints, for accommodation of the crystal lattice mismatch are invoked in the case of PZN-*x*PT compositions within the MPB [30–32], where intermediate adaptive ferroelectric phases are considered. Of interest are also PT-rich crystals, namely, far beyond the MPB. We note that in Brillouin scattering measurements of PZN-20.0PT crystals a sharp dip in the LA phonon frequency has been observed at 528 K [33], well above the $T_c = 503$ K. It has been attributed to a first-order ferroelectric phase transition from cubic-to-tetragonal symmetry and associated with "dynamic precursor microregions" forming in the high-temperature paraelectric phase. The latter are analogs of the PNRs, and $T_{\mathrm{wf}} = 528$ K may be typical for the PZN-20.0PT crystal. Although the PNRs are related to the microscopic compositional disorder with respect to the site occupancy by the heterovalent Zn^{2+} and Nb^{5+} cations, higher Ti-content may alter the matrix-nanodomain interface energies and modify the cubic-tetragonal phase transition temperature, T_{wf}. In fact, sample-dependent variations in the size and shape distribution of PNRs may also affect the T_{wf} at lower PT content, and even more so the AE intensity (Fig. 1) of the 500 K anomaly peaks.

In conclusion, strong AE bursts have been observed in PZN-*x*PT ($x = 0$–12%) crystals at a practically constant temperature $T_{\mathrm{wf}} \approx 500$ K for all values of x studied. T_{wf} corresponds to the characteristic 500 K temperature at which the PNR-related waterfall effect has been discovered at a wave vector $q_{\mathrm{wf}} \sim 0.2$ Å^{-1} from the zone center in the cubic phase of PZN-*x*PT crystals. We suggest that the AE activity generated at the T_{wf} temperature originates from local microscopic ferroelectric phase transitions within the growing in size PNRs when the latter reach a critical volume corresponding to the correlation length $\xi_c \sim$ 25–30 Å. Strong AE registered at 500 K implies martensitelike cubic-tetragonal ferroelectric transitions, typically followed by twinning. A sample calculation of the electrostrictive strain balance at the PNR boundary has been carried out for PZN-8.0PT to verify the feasibility of head-to-tail 90° twinning observed experimentally in PMN-*x*PT on a nanoscale. Similar investigations on PMN-*x*PT and other systems are underway, and the AE method may prove itself as a useful nondestructive diagnostic tool for studying the PNR-related phase transitions in relaxor ferroelectrics.

---

*Corresponding author.

[1] D. E. Cox, B. Noheda, G. Shirane, Y. Uesu, K. Fujishiro, and Y. Yamada, Appl. Phys. Lett. **79**, 400 (2001).

[2] Z. Kutnjak, J. Petzelt, and R. Blinc, Nature (London) **441**, 956 (2006).

[3] A. A. Bokov and Z.-G. Ye, J. Mater. Sci. **41**, 31 (2006).

[4] K. Hirota, S. Wakimoto, and D. E. Cox, J. Phys. Soc. Jpn. **75**, 111006 (2006).

[5] E. Dul'kin, I. P. Raevskii, and S. M. Emel'yanov, Phys. Solid State **45**, 158 (2003).

[6] E. Dul'kin, M. Roth, P.-E. Janolin, and B. Dkhil, Phys. Rev. B **73**, 012102 (2006).

[7] E. Dul'kin, M. Roth, B. Dkhiland, and J. M. Kiat, J. Appl. Phys. **98**, 023520 (2005).

[8] E. A. Dul'kin, Mater. Res. Innovations **2**, 338 (1999).

[9] D. La-Orauttapong, B. Noheda, Z.-G. Ye, P. M. Gehring, J. Toulouse, D. E. Cox, and G. Shirane, Phys. Rev. B **65**, 144101 (2002).

[10] P. M. Gehring, S.-E. Park, and G. Shirane, Phys. Rev. Lett. **84**, 5216 (2000).

[11] P. M. Gehring, S. Wakimoto, Z.-G. Ye, and G. Shirane, Phys. Rev. Lett. **87**, 277601 (2001).

[12] P. M. Gehring, S.-E. Park, and G. Shirane, Phys. Rev. B **63**, 224109 (2001).

[13] J. Hlinka, S. Kamba, J. Petzelt, J. Kulda, C. A. Randall, and S. J. Zhang, Phys. Rev. Lett. **91**, 107602 (2003).

[14] A. A. Bokov and Z.-G. Ye, Phys. Rev. B **66**, 064103 (2002).

[15] T. Iwase, H. Tazawa, K. Fujishiro, Y. Uesu, and Y. Yamada, J. Phys. Chem. Solids **60**, 1419 (1999).

[16] D. La-Orauttapong, J. Toulouse, J. L. Robertson, and Z.-G. Ye, Phys. Rev. B **64**, 212101 (2001).

[17] D. La-Orauttapong, J. Toulouse, Z.-G. Ye, W. Chen, R. Erwinand, and J. L. Robertson, Phys. Rev. B **67**, 134110 (2003).

[18] K. Ohwada, K. Hirota, P. W. Rehrig, Y. Fujii, and G. Shirane, Phys. Rev. B **67**, 094111 (2003).

[19] J. Toulouse, F. Jiang, O. Svitelskiy, W. Chen, and Z.-G. Ye, Phys. Rev. B **72**, 184106 (2005).

[20] Y. U. Wang, Phys. Rev. B **74**, 104109 (2006).

[21] D. Viehland, J. F. Li, and E. V. Colla, J. Appl. Phys. **96**, 3379 (2004).

[22] H. Wang, J. Zhu, N. Lu, A. A. Bokov, Z.-G. Ye, and X. W. Zhang, Appl. Phys. Lett. **89**, 042908 (2006).

[23] V. G. Gavrilyachenko, A. F. Semenchev, and E. G. Fesenko, Sov. Phys. Solid State **32**, 175 (1990).

[24] Y. Wang and A. G. Khachaturyan, Acta Mater. **45**, 759 (1997).

[25] H. Fan and H.-E. Kim, J. Appl. Phys. **91**, 317 (2002).

[26] E. G. Fesenko, V. G. Gavrilyachenko, A. F. Semenchev, and S. M. Yufatova, Sov. Phys. Solid State **27**, 719 (1985).

[27] M. J. Haun, E. Furman, S. J. Jang, H. A. McKinstry, and L. E. Cross, J. Appl. Phys. **62**, 3331 (1987).

[28] A. Lebon, H. Dammak, and G. Calvarin, J. Phys. Condens. Matter **15**, 3069 (2003).

[29] S.-F. Liu, S.-E. Park, L. E. Cross, and T. R. Shrout, J. Appl. Phys. **92**, 461 (2002).

[30] D. Viehland, J. Appl. Phys. **88**, 4794 (2000).

[31] Y. M. Jin, Y. U. Wang, A. G. Khachaturyan, J. F. Li, and D. Viehland, Phys. Rev. Lett. **91**, 197601 (2003); J. Appl. Phys. **94**, 3629 (2003).

[32] Y. U. Wang, Phys. Rev. B **73**, 014113 (2006).

[33] M. H. Kuok, S. C. Ng, H. J. Fan, M. Iwata, and Y. Ishibashi, Solid State Commun. **118**, 169 (2001).